VOL. 14, NO. 2, JANUARY 2019 ISSN 1819-6608
ARPN Journal of Engineering and Applied Sciences

www.arpnjournals.com

FINITE ELEMENT ANALYSIS OF REINFORCED CONCRETE DEEP BEAMS STRENGTHENED IN SHEAR WITH CFRP

Ahmed Abdullah Mansoor, Wisam D. Salman and Ali Lafta Abbas
Civil Engineering Department, Diyala University, Baquba, Iraq
E-Mail: aamansor2003@yahoo.com

ABSTRACT

A paper presents a numerical analysis using ANSYS finite element program to develop a model for expecting the performance of seven lightweight aggregate reinforced concrete deep beams with 28 days compressive strength 26MPa and density of 1950Kg/m^3 strengthened in shear by externally bonded CFRP. All beams have same dimensions (150mm width, 400mm depth and 1400mm length), longitudinal steel reinforcement ratio ρ=0.0115 and shear steel reinforcing Φ5@100mm. CFRP strips 50mm width are used for strengthening. The effective variable parameters were: a/d ratio, CFRP spacing, orientation and number of layers. The results obtained from the ANSYS finite element model got good agreement when compared to the experimental results [1] which were done for the same deep beams with the same material properties, internal reinforcement and strengthening schemes. The results show that the ultimate load and deflection predicted by numerical analysis is less than experimental results by 9% and 5.7% in average respectively. By using CFRP strips in shear strengthening, the ultimate load has increased by 18%, 13.6%, 32% and 27.3% for vertical, horizontal, inclined and double vertical layers, respectively for a/d=1. For a/d =0.8 the increase is 10% for vertical strips. It is recommended that the CFRP is placed such that the principal fiber orientation is either normal to the longitudinal beams axis or normal to the line joining the applied load and supports (strut path) to resist higher tensile stresses and strains distributed along it.

Keyword: lightweight aggregate concrete, deep beams, shear failure, finite element analysis, CFRP, strengthening.

INTRODUCTION

Reinforced concrete deep beams have been usually subject of significant interest in structural engineering applications. They are utilized as load conveying auxiliary components, for example, move supports utilized as a part of multistory structures to give segment balances or as flat stomachs, heap tops, establishment dividers, and seaward structures. They are additionally utilized as a part of development of fortifications, water tanks and canisters where the dividers go about as a vertical shaft crossing between the sections underpins and conveying a part of the floor stack.

Reinforced concrete beams are commonly classified as deep and shallow beams according to their shear span-to-depth ratio or clear span to overall depth. According to ACI 318M-14[2] deep beam has either: $l_c/h \leq 4.0$; or $a/h \leq 2.0$, where (l_c) is the clear span, (h) is the overall depth, and (a) is the shear span. In addition, profound pillar is characterized as part stacked on one face and upheld on the inverse face, with the goal that pressure struts can create between the heaps and the backings (Figure-1). Usually, the controlled strength of deep beams is shear rather than flexural strength, if normal amounts of longitudinal reinforcement are used, due to the small value of span to depth ratio.

Plane sections in deep beams do not remain plane after bending, so these beams could be considered as non-flexural beams. Also, their shear strength is significantly greater than that of slender beams because of the special capacity of the deep beams in redistributing internal forces before failure [3, 4].

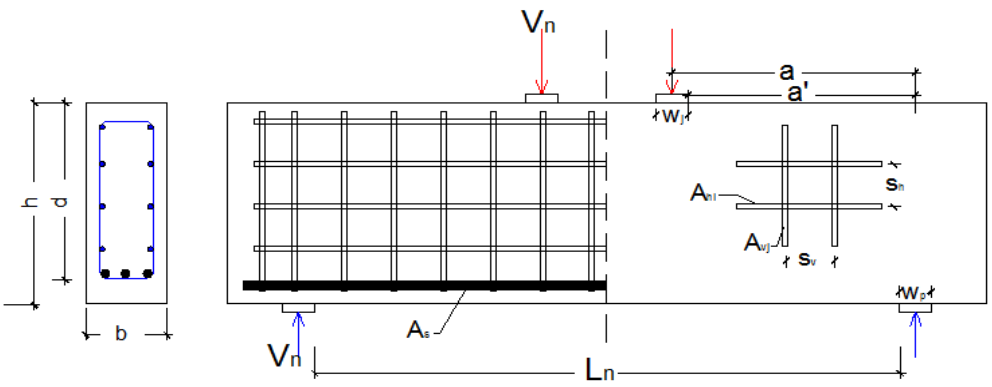

Figure-1. Typical deep beam [3].

The repair and strengthening of structurally deteriorated reinforced concrete deep beams are required to provide satisfactory resisting strength and serviceability. Deficiencies are usually the results of deterioration caused by service age and exposure to adverse environments, unexpected design load brought about by a growing society's results, different repair and strengthening techniques have been effectively developed to strengthen a structural constraction. In the most recent time, advancement of solid epoxy stick is prompted to a system that has extraordinary potential of overhauling buildings field.

Basically, the method contains bonding fiber reinforced polymer (FRP) plate or sheet, steel plates to the external surfaces of the structures concrete. FRPs play as composite materials with the concrete and assistances to transfer the externally applied loads [5]. The widely recognized kinds of FRP in the solid business are made with carbon, aramid or glass filaments. The FRPs are found as sheets, strips, wraps or covers.

The utilization FRPs to maintain and restore harmed structures has turned out to be progressively appealing because of its outstanding great mechanical properties, especially with its high quality to weight proportion and great exhaustion and erosion properties. Many experimental researches have presented that externally bonded FRP laminates could significantly upgrade the stiffness of structural members and the capacity of carrying load, developing the confinement and ductility to compression structural members as well as controlling the spread of cracks, increasing the flexural and shear capacities, [6- 9].

This research will be study the nonlinear behavior of shear critical deep beams (after being strengthened with CFRP strips which have been glued on the external surfaces of these deep beams) by using ANSYS. As well as, the enhancement in strength and stiffness, also the variation of the failure mechanism of the reinforced concrete beams due to CFRP are investigated.

EXPERMINTAL PROGRAM

The experimental program includes testing seven simply supported deep beams consisting of lightweight aggregate concrete with two-point loads(1). All the beams have the same dimensions of 1400mm length, 150mm width and 400mm depth. The a/d ratios are 0.8 and 1.0. The longitudinal reinforcement is 3Φ16mm (f_y =573MPa and f_u= 695Mpa) and the shear reinforcement is Φ5@100mm (f_y=476MPa and f_u= 578Mpa) in vertical and horizontal direction as shown in Figure-2). The compressive strength of concrete at 28 days is 26MPa and the dry density of about 1950kg/m^3. The two deep beams DBUSI and DBUS2 are a control beams and they haven't any strengthening. Table (1) shows the CFRP wrapping schemes for the analyzed deep beams and Figures (3) to (5) explains the arrangement of CFRP strips wrapping.

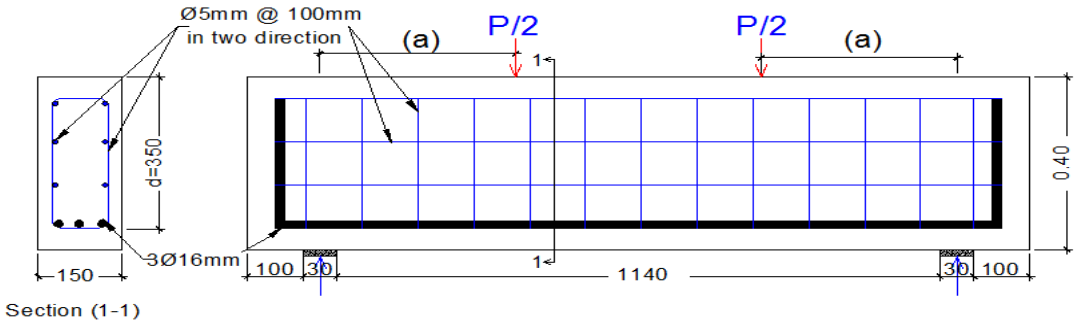

Figure-2. Typical deep beam dimensions and the reinforcement details.

Table-1. CFRP strengthening details.

Beam designation	a/d	CFRP strips details
DBUS1	1.0	None (control deep beam)
DBVS1		Strengthened with one-layer U-wrap vertical strips
DBHS1		Strengthened with one-layer horizontal strips
DBIS1		Strengthened with one-layer Inclined strips
DBVDS1		Strengthened with two layers U-wrap
DBUS2	0.8	None (control deep beam)
DBVS2		Strengthened with one-layer U-wrap vertical strips

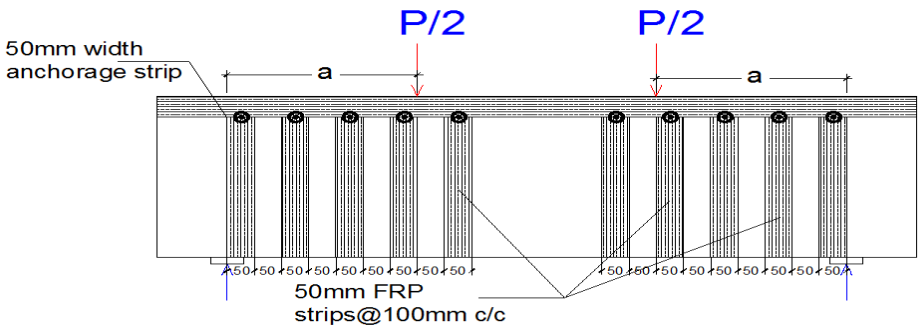

Figure-3. The arrangement of CFRP strips wrapping for DBVS1, DBVDS1 and DBVS2 Specimens.

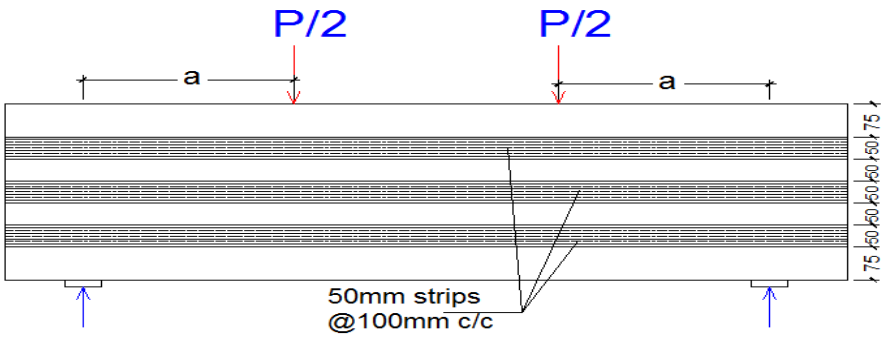

Figure-4. The arrangement of CFRP strips wrapping for DBHS1 specimen.

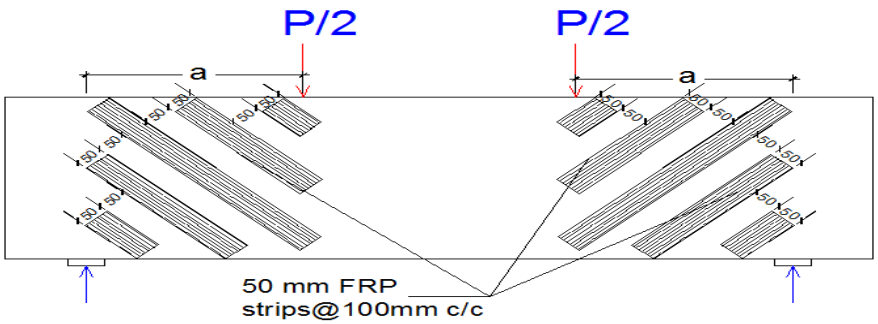

Figure-5. The arrangement of CFRP strips wrapping for DB1SI specimen.

MATERIAL MODELING

Concrete model

The relationship of stress-strain of concrete is different in tension than in compression region as it was a nonlinear material. Tensile strength of concrete is usually around 8-15% of the compressive strength [10]. In ANSYS, the behavior of concrete stress-strain can be considered by using Drucker–Prager or von-Mises yield principle. According to Desayi and Krishnan [11], the concrete stress-strain curve used in equations (1) and (2), is defined by a piecewise linear mathematical term. These two equations were used along with equation (3) accepted by Gere and Timoshenko [12] to concept the stress-strain curve for uniaxial compressive concrete in this study.

$$f_c = \frac{\varepsilon E_c}{1+\left[\frac{\varepsilon}{\varepsilon_0}\right]^2} \quad \text{for } \varepsilon_1 \le \varepsilon \le \varepsilon_0 \tag{1}$$

$$\varepsilon_0 = \frac{2\,f'_c}{E_c} \quad \text{for } \varepsilon_0 \le \varepsilon \le \varepsilon_{cu} \tag{2}$$

$$f_c = \varepsilon\, E_c \quad \text{for } 0 \le \varepsilon \le \varepsilon_1 \tag{3}$$

$$f_c = f'_c \quad \text{for } \varepsilon_0 \le \varepsilon \le \varepsilon_{cu} \tag{4}$$

where:

$\varepsilon_1 =$ *the strain corresponding to* $0.3f'_c = 0.3f'_c/E_c$
$f_c =$ stress at any strain ε (MPa)
$\varepsilon =$ strain at stress f_c,
$\varepsilon_0 =$ strain at the ultimate compressive strength f'c.
Ec= 17850MPa is taken from experimental results.

In the present research, the concrete was assumed to be a homogenous and initially isotropic material. Figure-6 demonstrates the disentangled compressive uniaxial stress-strain relationship that was utilized as a part of this study for each specimen. It can be seen that the stress-strain curve for concrete is linearly elastic up to about 30% of the maximum compressive strength. Beyond this point, the stress growths regularly till to the maximum compressive strength σ_{cu}. After that, the curve inclines into a softening region, and finally crushing failure happens at an ultimate strain ε_{cu}. On contrasts, the stress-strain curve for concrete in tension is nearly linearly elastic up to the maximum tensile strength. After that point, the concrete cracks and the strength decreases regularly to zero.

Steel reinforcement modeling

Figure-7 shows the stress-strain relationship used in this study. In general, steel was thought to be a versatile splendidly plastic material and identical in tension and compression. Elastic modulus Es= 200,000MPa and Poisson's ratio of 0.3 was used in this study.

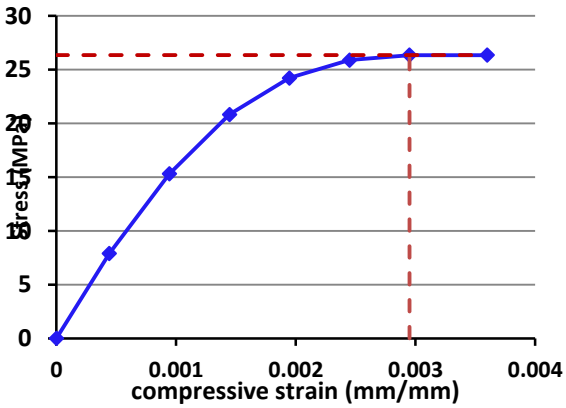

Figure-6. Uniaxial stress-strain relationship for lightweight concrete of present study.

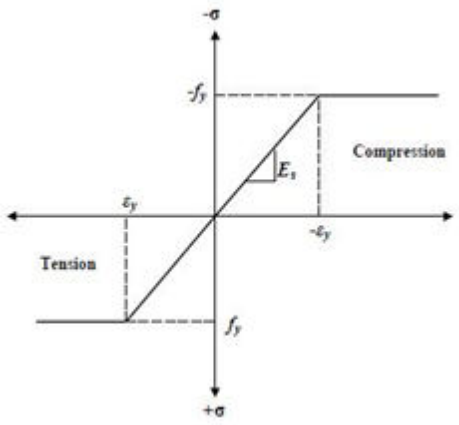

Figure-7. Stress-strain curve for steel reinforcement [13].

FRP composites modeling

Linear elastic properties for the CFRP composites were expected all through this study as shown in Figure-8. The unidirectional CFRP composite truly shows perpendicular behavior, however it was demonstrated that exclusive axial modulus is significance in a utilization of this sort. It is reasonable to model CFRP strips as an isotropic material rather than orthotropic since they are exposed to tensile forces.

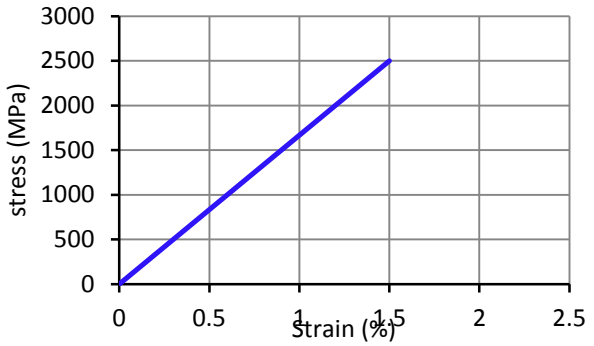

Figure-8. Stress-strain curve for CFRP composite in the direction of the fiber.

FINITE ELEMENTS MODELING

ANSYS program (version 15) has been used to doing finite element modeling. Solid65, has been depend to model the lightweight aggregate concrete. The solid65 element has 8 nodes with 3 degrees of freedom at each node-translations in the nodal x, y and z directions. The element is accomplished of plastic deformation, cracking in three orthogonal directions, and crushing. The node locations and geometry for the element type is shown in Figure(9-a).

LINK180 element has been depend to model the longitudinal reinforcement and shear reinforcement. It is a uniaxial tension-compression member that can consist of nonlinear material properties. The element includes two nodes with three degrees of freedom at each one. Figure (9-b) shows the coordinate system, geometry and node locations for this element.

Soild185 finite element has been used to model the steel plates were added at support locations and under the two applied load points. This element is defined by four nodes with three degrees of freedom at each node: translations in the nodal x, y, and z directions (Figure 9-c). The steel plate was assumed to be a linear elastic material with a Poisson's ratio of 0.3 and elastic modulus of 200GPa.

SOLID41 layered structural solid element has been depend to model the CFRP materials. The element comprises 8 nodes with three degrees of freedom at each node. The element material is assumed to be orthotropic and no slippage is assumed between the element layers (perfect interlaminate bond). The stress-strain relationships for the CFRP laminates assumed linearly elastic in this study. The element is shown in Figure (9-d).

The thickness of the CFRP strips (in case of one layer) is 0.16 mm.

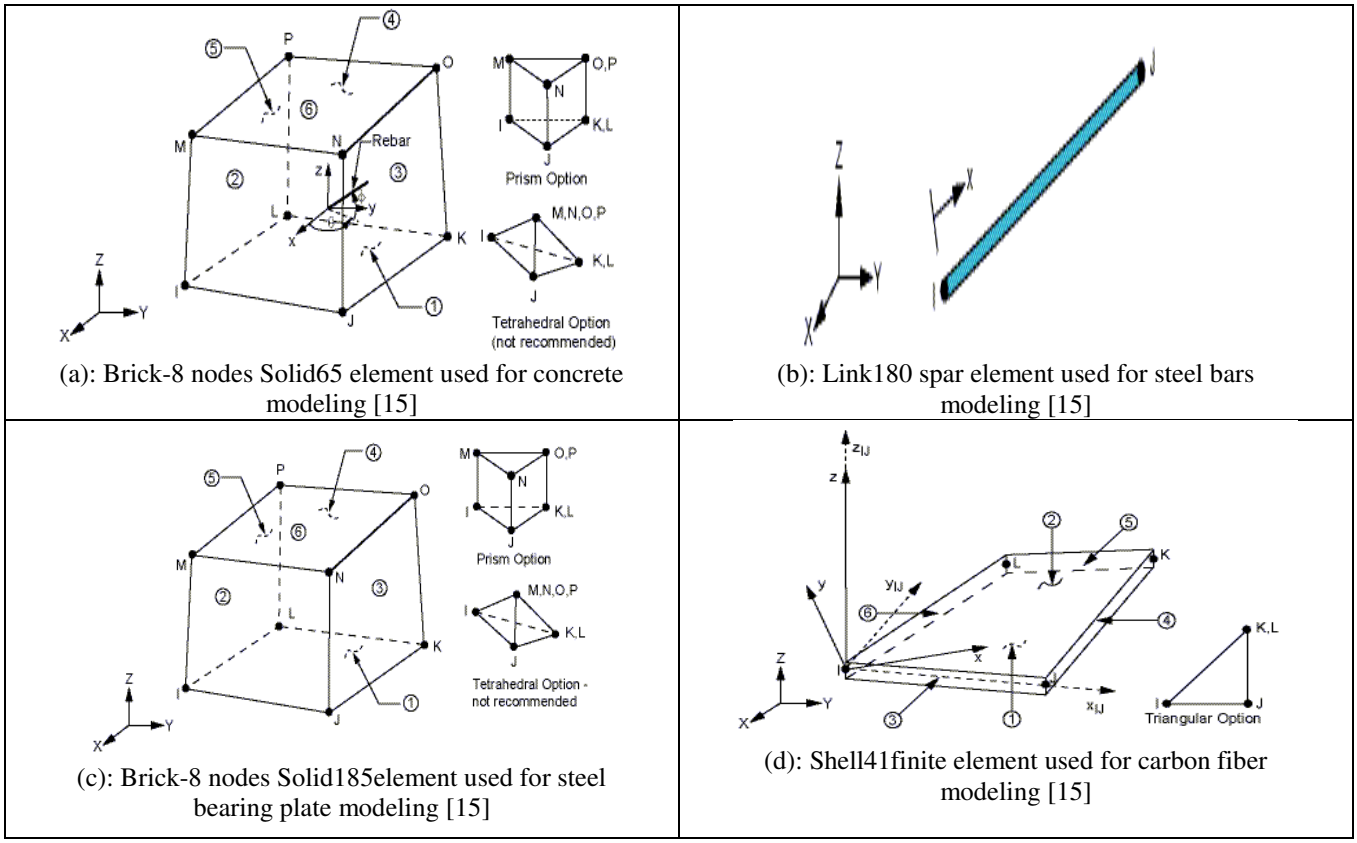

(a): Brick-8 nodes Solid65 element used for concrete modeling [15]

(b): Link180 spar element used for steel bars modeling [15]

(c): Brick-8 nodes Solid185element used for steel bearing plate modeling [15]

(d): Shell41finite element used for carbon fiber modeling [15]

Figure-9. Elements used for modeling the deep beams.

MATERIAL PROPERTIES

ANSYS requires the following data to be input for the concrete properties: f'_c =26MPa, f_r = 3.12 MPa, E_c=17850 MPa, these values have been calculated from an experimental work done for the same deep beams with the same properties. Poisson's ratio (v_c) has been taken as 0.15. The coefficients for the open and closed cracks (β_o), (β_c) were taken 0.1 and 0.8, respectively.

The internal main and the shear reinforcement steel bars has been modeled by Link180 which has been assumed to be bilinear isotropic. Linear elastic properties of CFRP composite materials has been assumed as shown in Figure-8 with modulus of elasticity and ultimate tensile strength 230 GPa and 3900 MPa respectively. Poison ratio for CFRP has been taken as 0.3. Perfect bond has been assumed between carbon fiber and concrete so as the two materials shared the same nodes.

DEEP BEAMS MESHING

The meshing for the analyzed deep beams is shown in Figure-10-a, while Figure-10-b shows the typical steel reinforcement modeling. There are 56 elements along the length of beam, 8 elements along depth and 6 elements along width. Figure-11 shows the configuration of FRP layers elements.

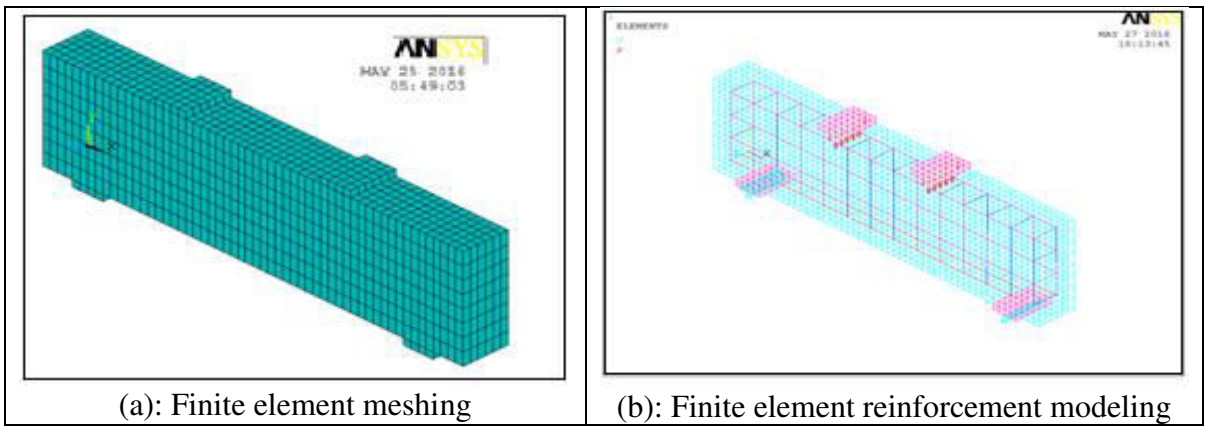

Figure-10. FEM modeling for the analyzed deep beam.

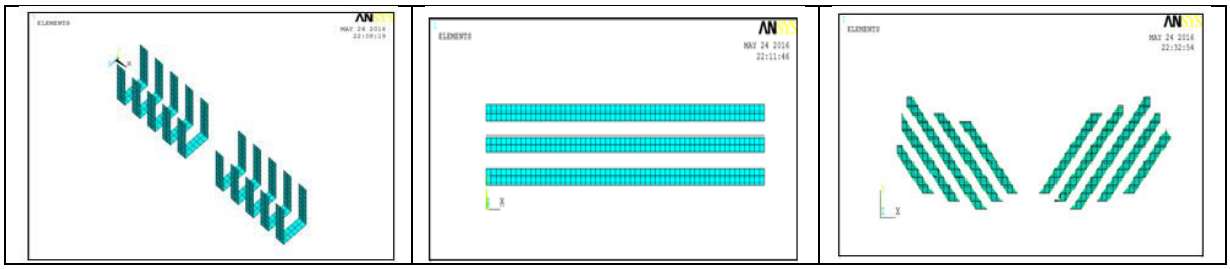

Figure-11. FRP layered solid elements configuration.

LOADS AND BOUNDARY CONDITIONS

Figure-12 explains the boundary conditions of all tested specimens. The hinge support at the right-hand side of the deep beams has been simulated by single lines of nodes constrained in the UY, and UX directions. to simulate the roller support on the left hand side of the beams, the DOF in the UY has been taken to be zero.

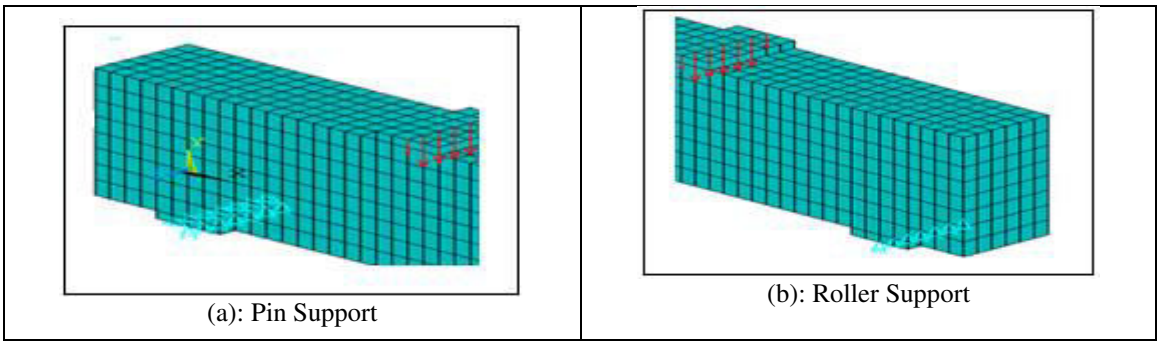

Figure-12. Applied loads and support boundary conditions in ANSYS model.

RESULTS AND DISCUSSIONS

In order to validate the numerical representation of the lightweight aggregate reinforced concrete deep beams strengthened in shear with CFRP strips, the results of the finite element representation are compared to the experimental results. The comparison results are as follow:

Failure load

Table-3 illustrates a comparison between the ultimate loads obtained from the finite element analysis with the corresponding experiential loads. This table shows also the difference between the experimental and numerical results. It is observed that the obtained load values from the numerical analysis was close for DBUS1 and DBISI but they are somewhat less than that of the experimental one by 9% on average for the remain specimens.

Table-2. Comparison between the ultimate loads from the experimental tests FE analysis.

Deep Beam No.	a/d	ultimate load (kN)		% difference
		$(P_u)_{FEM.}$	$(P_u)_{Exp}$	
DBUS1	1.0	437	440	0.7
DBVS1		486	520	6.5
DBHS1		465	500	7.0
DBIS1		577	580	0.52
DBVDS 1		530	560	5.4
DBUS2	0.8	525	620	15.32
DBVS2		608	680	10.6

Deflected shapes

Table-4 shows a comparison between the midspan deflection for the experimental ($\delta_{vExp.}$) and the finite element models (δ_{vFEM}) results, both are measured at ultimate load. Also Figures (13) and (14) shown the mid deflection for the experimental and the finit element models for seven specimens. It can be seen the well agreement between the finite element analysis and the experimental results within maximum percentage different of 5.7% in average.

It can be considered that the critical diagonal crack in a reinforced concrete deep beam as a crack governed by shear rather than by bending as its atarting is very close to the support. The deflected shapes of the finite element analysis of the analyzed deep beam specimens at ultimate loads are shown in Figure-15.

Table-3. Comparison between max. deflections of the exp. and FE analysis at failure load.

Deep beam No.	a/d	Central deflection (mm)		% difference
		$(\delta_v)_{Exp.}$	$(\delta_v)_{FEM.}$	
DBUS1	1	8.2	8.57	4.5
DBVS1		2.85	2.59	9.12
DBHS1		8.3	8.95	7.8
DBIS1		7.5	7.35	2
DBVDS1		7.1	7.40	4.2
DBUS2	0.8	7.4	8.08	9.19
DBVS2		8.26	8.5	2.91

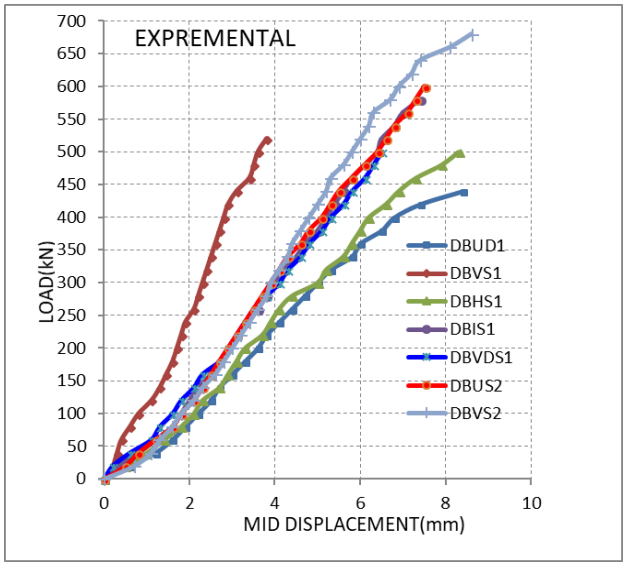

Figure-13. Experimental load-mid deflection shapes for specimens.

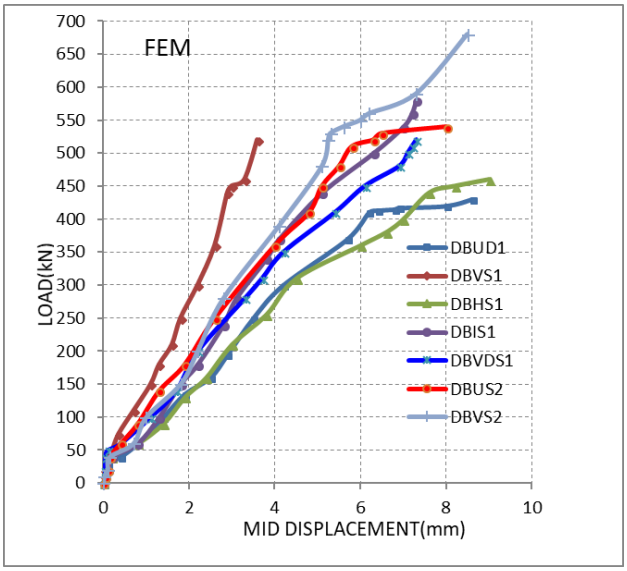

Figure-14. Finite element models for load-mid deflection shapes for specimens.

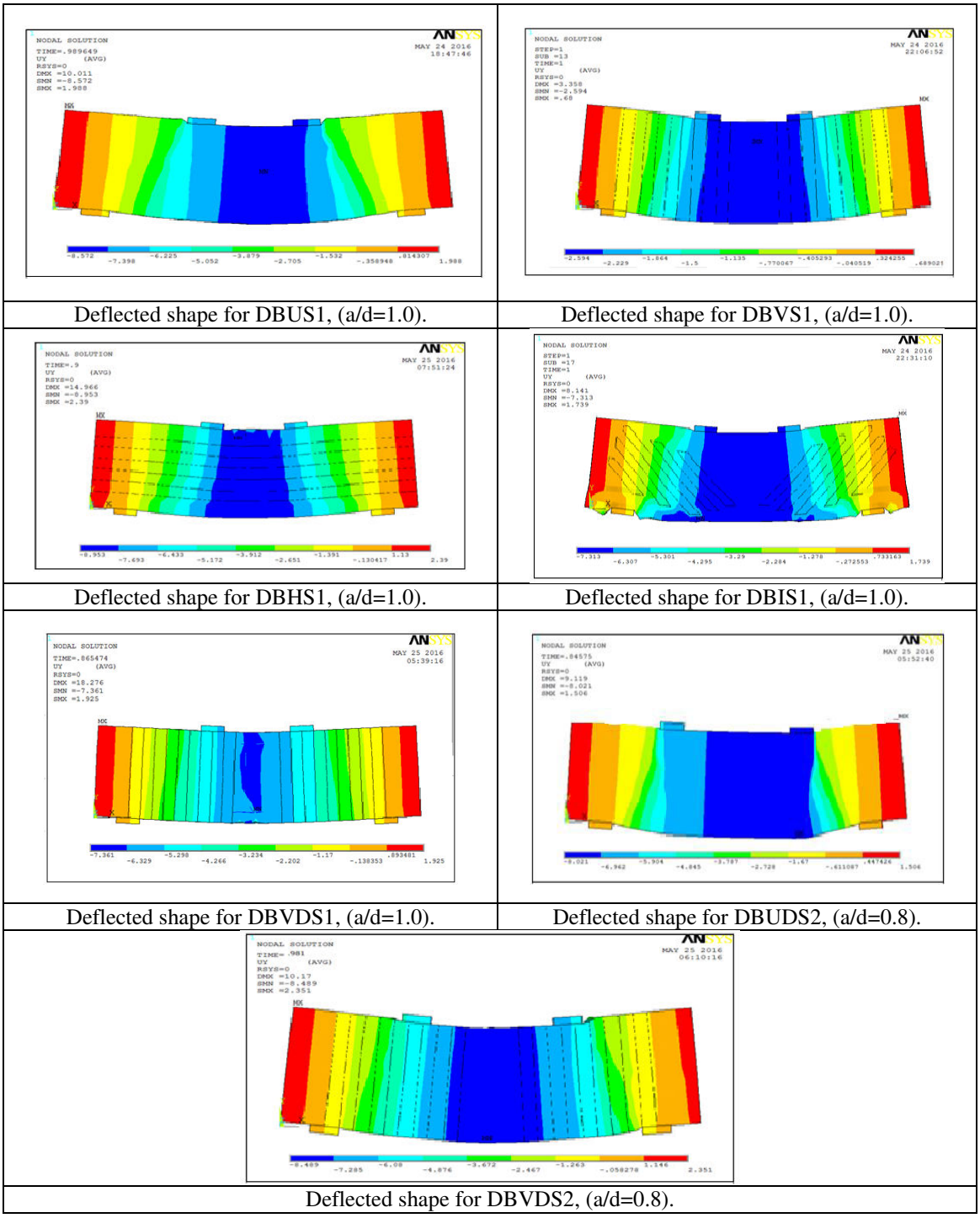

Figure-15. Deflected shapes for the analyzed deep beams.

Stress and strain distributions

Figures (16) and (17) explain distributions of the normal stress of concrete in x-direction (Sx) and the principal stress for specimen DBUS1 at the ultimate load respectively. It can be seen that the maximum compressive stresses are created generally at the mid-span zone (along strut path).

Figures (18) and (19) clarify, respectively, the nominal stresses and strains growth in the vertical strips of the strengthened deep beam DBVS1 (fortified by one-layer vertical strips). It can be seen that the maximum qualities for the tensile stresses are in the second and third strips and they mimicked fit the bottle shaped state of the strut path. This pattern is like what was noticed for the concrete strain in the experimental work where the maximum tensile stress and strains have been disseminated along the strut path.

Figures (20) and (21) clarify the stress and strain distributions in the horizontal CFRP strips used to strength DBHS1. The higher tensile strength has been noticed in

the primary strip in around the mid of the shear traverse zone close to the base face of the specimen being around (950MPa). The second higher stress values have appeared in the second strip.

Growth of the tensile stresses in the CFRP strips for the specimens DBISI, DBVDSI, DBVS2 could be seen in Figures (22) to (24), respectively.

All the figures explain that the strain information of CFRP got from finite element analysis and the experimental information for the tested specimens have comparative propensities firstly, wherever the greatest estimations of the strains are also gathered practically in the mid height region of the deep beam which is adequate the bottle formed dispersion of the strains. Also, it can be notified that the strains proposed by the experimental results are greater than those for the finite element analysis; this might be according to imprecision of the information materials properties for the model.

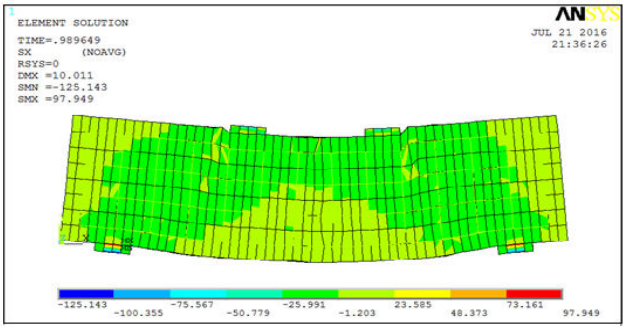

Figure-16. Variation in concrete normal stresses of the unstrengthened deep beam DBUS1, a/d=1.0 along the longitudinal axis.

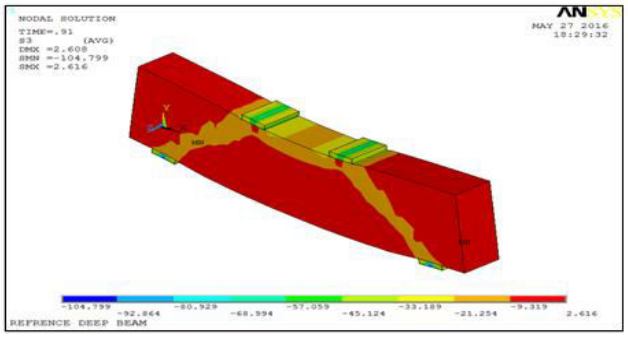

Figure-17. Finite element principal stresses of the unstrengthened deep beam DBUS1, a/d=1.0.

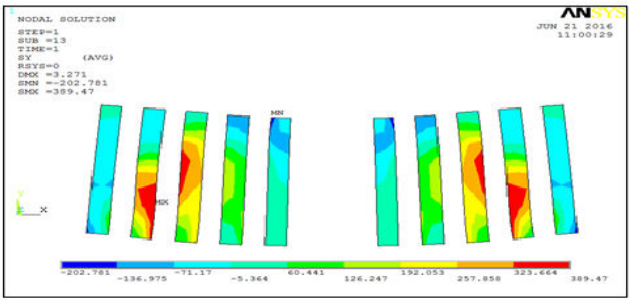

Figure-18. Finite element normal stresses in the vertical strips of deep beam DBVS1, a/d=1.0.

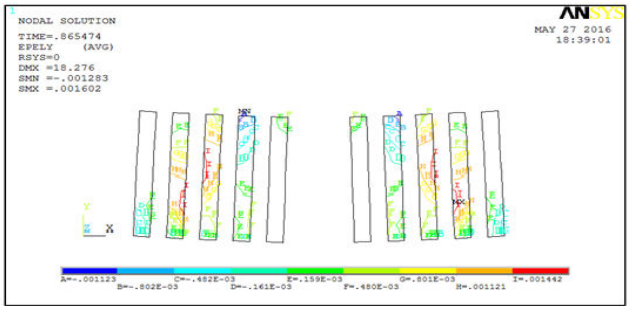

Figure-19. Finite element normal strains in the vertical strips of deep beam DBVS1, a/d=1.0.

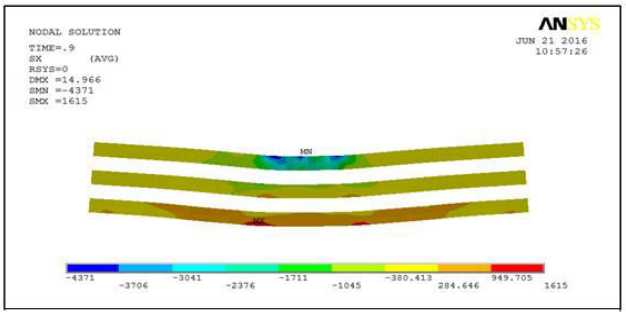

Figure-20. Finite element normal stresses in the horizontal strips of deep beam DBHS1, a/d=1.0.

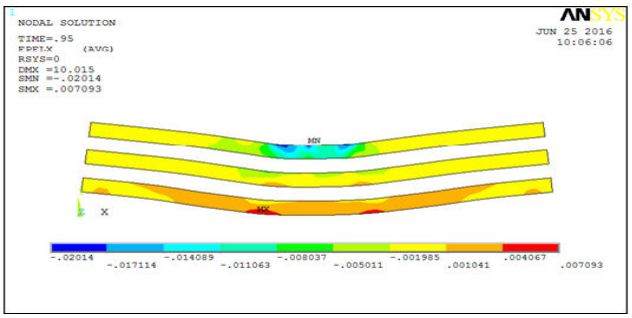

Figure-21. Finite element normal strain in the horizontal strips of deep beam DBHS1, a/d=1.0.

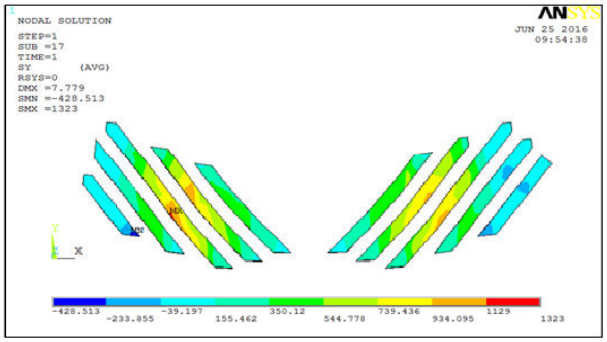

Figure-22. normal stresses in inclined strips of the DBIS1 (strengthened with one layer inclined strips with different length) a/d=1.0.

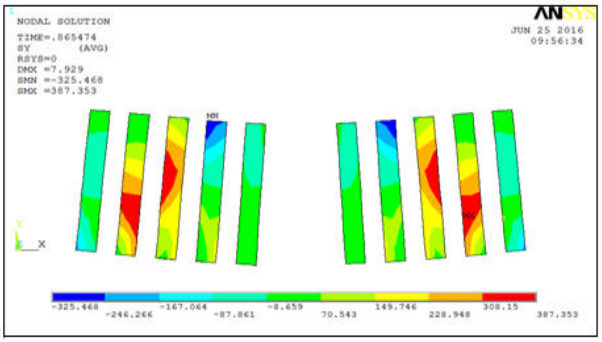

Figure-23. Finite element normal stresses in the vertical strips of deep beam DBVDS1 (strengthened by two layers vertical strips), a/d=1.0.

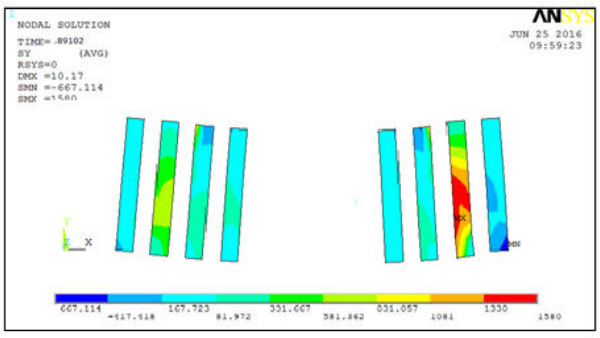

Figure-24. Finite element normal stresses in the vertical strips of deep beam DBVS2 (strengthened by one layers vertical strips), a/d=0.8.

CONCLUSIONS

a) The finite element models used ANSYS program are effective and accurate to expect the behavior of CFRP externally bonded to strengthening lightweight aggregate reinforced concrete deep beams.

b) Results show that the ultimate load predicted by finite element analysis is less than experimental results by 9% on average.

c) Also, the results show that the deflection predicted by finite element analysis is less than experimental results by 5.7% on average.

d) By using CFRP strips in shear strengthening, the ultimate load has increased by 18%, 13.6%, 32% and 27.3% for vertical, horizontal, inclined and double vertical layers, respectively for a/d=1. For a/d =0.8 the increase is 10% for vertical strips.

e) By using CFRP strips in shear strengthening, the deflection has decreased by 56%, for inclined a/d=1. For a/d =0.8 the decrease is 68% for vertical strips.

f) For the higher a/d ratio, the vertical arrangement for CFRP strengthening strips is highly efficient and improves the shear strength of the lightweight reinforced concrete deep beams in comparison with the horizontal one.

g) FRP scheme in the shear span is significantly postponed the creation of diagonal shear cracks and providing confident limitation to the succeeding development of cracks.

h) It is recommended that the CFRP is placed such that the principal fiber orientation is either normal to the longitudinal beams axis or normal to the line joining the applied load and supports (Strut path) to resist higher tensile stress and strains distributed along it.

REFERENCES

[1] Sarsam K.F.; Al-Bayati N.M. and Mohammed A.S. Effect of Shear Span-Depth Ratios on Shear Strengthening of Porcelanite Lightweight Aggregate Reinforced Concrete Deep Beams Strengthened Externally By bonded CFRP Strips. accepted for publication in Engineering and Technology Journal, University of Technology, Baghdad, Iraq.

[2] ACI Committee 318. 2014 Building Code Requirements for Structural Concrete (ACI 318M-14) and Commentary on Building Code Requirements for Structural Concrete (ACI 318R-14). American Concrete Institute, Farmington Hill, MI. p. 524.

[3] Russo G.; Venir R. and Pauletta M. 2005. Reinforced Concrete Deep Beams-Shear Strength Model and Design Formula. ACI Structural Journal. 102(3): 429-437.

[4] Azam R. 2010. Behavior of Shear Critical RC Beams with Corroded Longitudinal Steel Reinforcement.

MSc. Thesis, University of Waterloo, Civil Engineering, Canada. p. 121.

[5] Valerio P. 2009. Realistic Shear Assessment and Novel Strengthening of Existing Concrete Bridges. PhD Thesis, Department of Architecture and Civil Engineering, University of Bath. p. 240.

[6] Chin S.C.; Shafiq N. and Nuruddin M.F. 2012. Strengthening of RC Beams with Large Openings in Shear by CFRP Laminates: 2D Nonlinear FE Analysis. International Journal of Civil and Environmental Engineering. 6: 195-200.

[7] Khalifa A. and Nanni A. 2000. Improving Shear Capacity of Externally RC T-Section Beams Using CFRP Composites. Cement and Concrete Composites. 22(2): 165-174.

[8] Izzet A.F. 2008. Retrofit Of Shear Critical RC Beams With Carbon Fiber Reinforced Polymer Sheets. PhD Thesis, University of Technology/ Building and Construction Department, Baghdad, Iraq. p. 176.

[9] Parth Athawale B.E. 2012. Analysis of Factors Affecting Effective Bond Length for Fiber Reinforced Polymer Composite Laminate Externally Bonded to Concrete Substrate. MSc. Thesis, Texas Technical University. p. 116.

[10] Kachlakev D.; Miller T. and Yim S. 2001. Finite Element Modeling of Reinforced Concrete Structures Strengthened with FRP Laminates. Final Report, Oregon Department of Transportation, Research Group and Federal Highway Administration, Washington, DC 20590. pp. 113.

[11] Desayi P. and Krishnan S. 1964. Equation for The Stress-Strain Curves of Concrete. ACI Journal. 61(3): 345-350.

[12] Gere J.M. and Timoshenko S.P. 1997. Mechanics of Materials. PWS Publishing Company, Boston, Massachusetts, 4th edition.

[13] Subramani T.; Manivannan R. and Kavitha M. 2014. Crack Identification in Reinforced Concrete Beams Using ANSYS Software. Journal of Engineering Research and Applications, ISSN : 2248-9622, 4(6): 133-141.

[14] Kwak H.G.; Filippou C.F. 1990. Finite Analysis Concrete of Reinforced Concrete Structures under Monotonic Loads. A Report on Research Conducted under Grant, RTA-59M848, Mechanics and Materials Department, Civil Engineering, University of California, Berkeley. p. 124.

[15] ANSYS-Release Version 15.0. 2015. ANSYS Help. Copyright.